Journal of Medicinal Chemistry

ARTICLE

pubs.acs.org/jmc

Evolution of Potent and Stable Placental-Growth-Factor-1-Targeting CovX-Bodies from Phage Display Peptide Discovery

Kristen E. Bower,[*,†] Son N. Lam,[*,†] Bryan D. Oates, Joselyn R. del Rosario, Emily Corner, Trina F. Osothprarop, Arvind G. Kinhikar, Julie A. Hoye, R. Ryan Preston, Robert E. Murphy, Lioudmila A. Campbell, Hanhua Huang, Judith Jimenez,[‡] Xia Cao,[‡] Gang Chen, Zemeda W. Ainekulu, Aakash B. Datt, Nancy J. Levin, Venkata R. Doppalapudi, Steven R. Pirie-Shepherd, Curt Bradshaw,[§] Gary Woodnutt, and Rodney W. Lappe

CovX Research, Pfizer, Inc., 9381 Judicial Drive, Suite 200, San Diego, California 92121, United States

Supporting Information

ABSTRACT: Novel phage-derived peptides are the first reported molecules specifically targeting human placental growth factor 1 (PlGF-1). Phage data enabled peptide modifications that decreased IC_{50} values in PlGF-1/VEGFR-1 competition ELISA from 100 to 1 μM. Peptides exhibiting enhanced potency were bioconjugated to the CovX antibody scaffold **1** (CVX-2000), generating bivalent CovX-Bodies with 2 nM K_D against PlGF-1. In vitro and in vivo peptide cleavage mapping studies enabled the identification of proteolytic hotspots that were subsequently chemically modified. These changes decreased IC_{50} to 0.4 nM and increased compound stability from 5% remaining at 6 h after injection to 35% remaining at 24 h with a β phase half-life of 75 h in mice. In cynomolgus monkey, a 78 h β half-life was observed for lead compound **2**. The pharmacological properties of **2** are currently being explored.

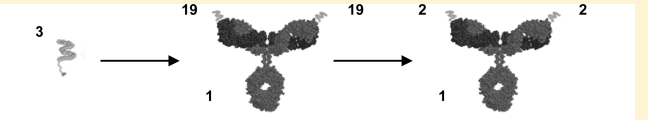

Cmpd	IC_{50} (nM)	Sequence	β-$t_{1/2}$ (Hrs)
3	100,000	Y D I C H Y I R L P H C F A V	-
19	2	F D V C K W V T L P H C K V M K_{AZD}	-
2	0.4	ADAA F E_{Me} V C H Y I K_{AZD} L Aib H C t K_{Ac} Aib	75

INTRODUCTION

Peptides can be potent therapeutic pharmacophores but exhibit short in vivo half-lives attributed to rapid renal clearance and serum proteolysis.[1] In contrast, therapeutic antibodies exhibit prolonged pharmacokinetics conferred via FcRn-mediated recycling, but antibodies can face cross-reactivity issues when raised against antigens highly homologous to other naturally occurring proteins.[2] The limitations of both can be resolved with the development of a CovX-Body,[3,4] a unique bioconjugate consisting of peptides or other pharmacophores stably linked through an AZD linker (Figure 1a) to proprietary antibody scaffold **1** (Figure 1b). An optimized CovX-Body retains or improves the biological and pharmacological properties of its parent molecules while demonstrating enhanced in vivo stability. Here we describe the sequential incorporation of several complementary pharmacophore optimization strategies in the development of **2**, a CovX-Body targeting PlGF-1 (Figure 1c).

PlGF is a pleiotropic member of the VEGF family with multiple suggested roles in cancer.[5,6] In contrast to VEGF, which exerts biological effects primarily through VEGF receptor 2 (VEGFR-2/Flk-1), PlGF proteins interact uniquely as high-affinity homodimers with VEGF receptor 1 (VEGFR-1/Flt-1).[6−8] This induces dimerization and cross-phosphorylation of receptors, downstream signaling, and receptor internalization.[7−9] Human PlGF-1 interacts only with VEGFR-1; PlGF-2 is a longer splice variant containing a 21-residue heparin binding domain that can recruit neuropilin-1/2 via heparin in a cell- and tissue-specific manner.[8−10] Mice only express a homologue to human PlGF-2, which interacts with heparin and neuropilins.[5]

A neutralizing antibody specifically targeting mouse PlGF (α-PlGF) demonstrated efficacy in several syngeneic tumor models, complemented anti-VEGF therapies, and did not induce the angiogenic escape program associated with these therapies.[11] A second mAb targeting human PlGF-1 and -2 demonstrated efficacy in a DanG xenograft model.[12] In contrast, four different antibodies inhibiting both mPlGF and hPlGF-2 had no significant effect on tumor growth or angiogenesis in 15 different tumor models and did not complement anti-VEGF therapy.[13] Genetic ablation of the VEGFR-1 tyrosine kinase domain also failed to inhibit anti-VEGF-A sensitive or resistant tumors, contrasting prior reports of antitumor activity for anti-VEGFR-1 therapies.[14,15]

To fully understand the mechanism of action for PlGF and its potential suitability as a cancer target, it may be necessary to consider the specific roles of the individual PlGF proteins. However, none of the previously reported molecules target PlGF-1 without cross-reacting with PlGF-2. **2** targets human PlGF-1 with 100-fold specificity over that for PlGF-2 or mouse PlGF. It represents a complementary tool that, together with the previously reported antibodies, should permit a more complete delineation of PlGF biology and pharmacology than previously feasible. Moreover, the pharmacophore optimization strategies

Received: September 21, 2010
Published: January 31, 2011

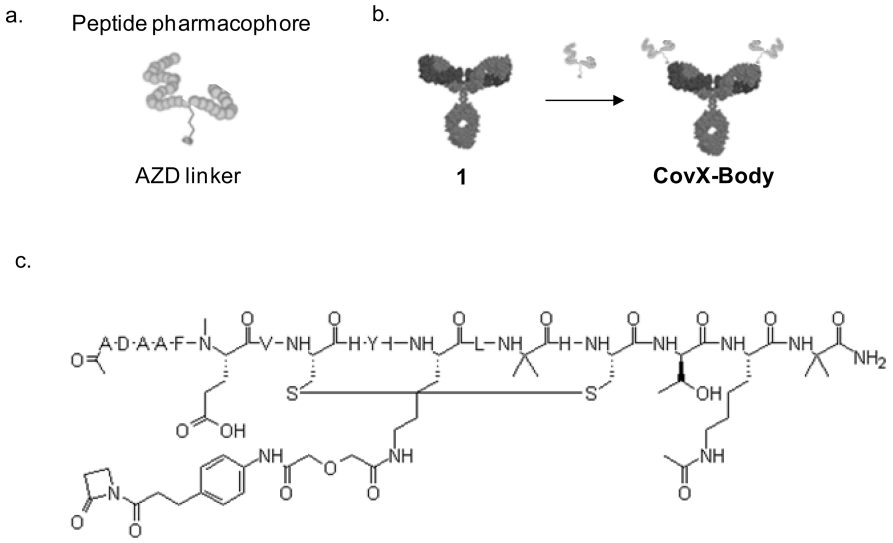

Figure 1. The generation of a CovX-Body is shown. (a) Pharmacophores are first activated via attachment of an AZD linker. (b) Activated pharmacophores are bioconjugated to proprietary antibody scaffold **1** to generate bivalent CovX-Bodies. (c) The structure of the AZD-conjugated peptide pharmacophore of CovX-Body **2** is shown.

Table 1. Evolution of PlGF-Binding Peptides Identified from Phage Display

compd	IC_{50} (μM)	1	2	3	4	5	6	7	8	9	10	11	12	13	14	15
3	100	Y	D	I	C	H	Y	I	R	L	P	H	C	F	A	V
4	100	L	D	V	C	L	W	V	S	L	P	H	C	L	A	I
5	100	W	Q	I	C	D	I	L	T	L	P	H	C	I	F	N
6	9	Y	D	I	C	K	Y	I	R	L	P	H	C	R	A	V
7	9	Y	D	I	C	K	Y	I	R	L	P	H	C	K	A	V
8	19	F	M	V	C	N	Y	V	T	L	P	W	C	P	M	Q
9	9	F	D	V	C	N	W	V	G	L	P	H	C	R	V	M
10	>10000	F	D	V	C	N	W	V	G	A	P	H	C	R	V	M
11	5	F	D	V	C	N	W	V	G	L	A	H	C	R	V	M
12	>10000	F	D	V	C	N	W	V	G	L	P	A	C	R	V	M
13	6	F	D	V	C	K	W	V	G	L	P	H	C	K	V	M
14	5	F	D	V	C	K	W	V	T	L	P	H	C	R	V	M
15	1	F	D	V	C	K	W	V	T	L	P	H	C	K	V	M
16	1	F	D	V	C	N	W	V	T	L	P	H	C	K	V	M
17	1	F	D	V	C	K	W	V	T	L	P	H	C	K	M	Q
18	1	F	D	V	C	N	W	V	T	L	P	H	C	K	M	Q

described here may be broadly applicable in the development of peptide-based therapeutics.

RESULTS

PlGF-Binding Peptides Identified in Phage Display Are Competitive Inhibitors of VEGFR-1. A phage screen was conducted using cyclic and linear peptide libraries to identify molecules that could bind PlGF-1 and inhibit the PlGF-1/VEGFR-1 interaction. Three disulfide-bridged hits (**3**, **4**, and **5**, 100 μM) were identified (Table 1); all three contained a conserved CXXXXLPHC motif. Hits were subjected to site-specific saturation mutagenesis to identify changes that increased potency. The presence of Lys5 in combination with Arg13 or Lys13 within the **3** sequence contributed to enhancement of peptide antagonist activity that resulted in IC_{50} values as low as 9 μM (**6** and **7**).

Concurrently, two new peptides with IC_{50} values of 19 and 9 μM were identified from additional screens (**8** and **9**). Alanine scanning of the LPH motif revealed Leu9 and His11 within the **9** peptide to be critical for antagonist activity (**10**, **11**, and **12**, Table 1). Lys5 and Lys13 incorporation into **9** (**13**) retained antagonist activity, as did incorporation of the Thr8 present in **8** (**14**). Combining favorable residues from **8**, **9**, **13**, and **14** afforded four peptides (**15**−**18**) that inhibited the PlGF/VEGFR1 interaction with IC_{50} of 1 μM (Table 1).

CovX-Body 19 Binds PlGF-1 with 3 log Potency Increase over Its Parent Peptide. A competitive binding ELISA was used to evaluate relative peptide potencies (Figure 2a). Consistent with the known binding constant of PlGF/VEGFR-1 interactions,[16] the IC_{50} of soluble VEGFR-1 (sVEGFR-1) was approximately 400 pM. Peptide **15**, exhibiting a 1 μM IC_{50} value, was selected for conjugation to the **1** scaffold. **15** was tethered with an azetidin-2-one (AZD) linker at its N- or C-terminus. For N-terminal tethering, the tether was attached directly onto the Phe1 α-amine. C-Terminal tethering required

dx.doi.org/10.1021/jm101226k | J. Med. Chem. 2011, 54, 1256–1265

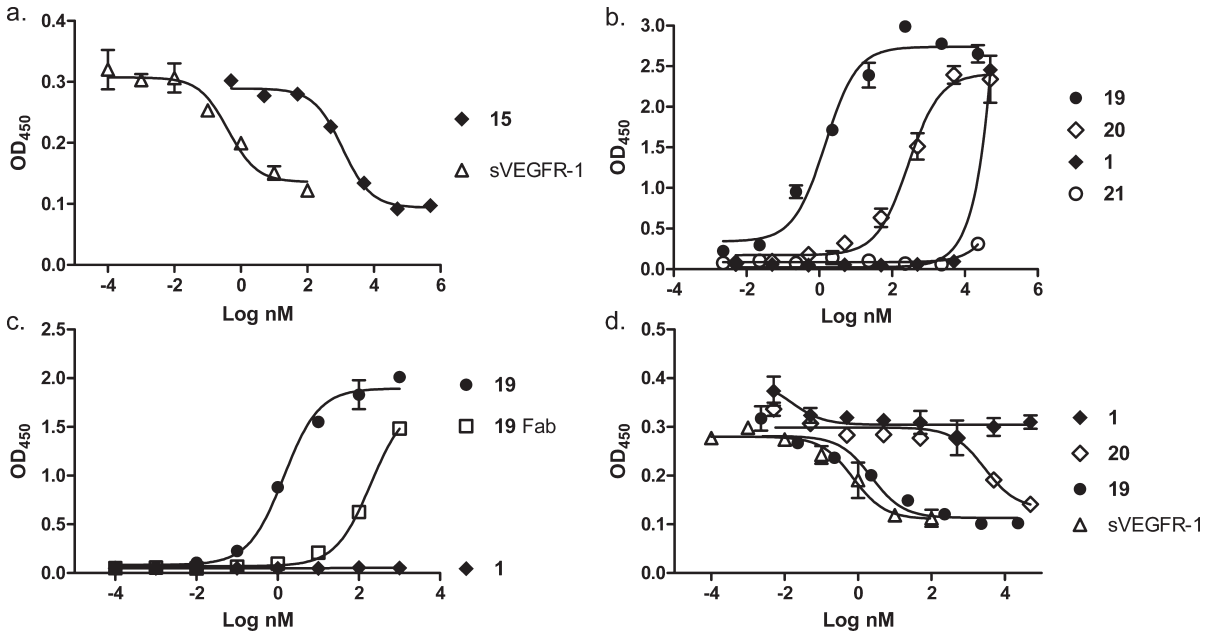

Figure 2. CovX-Body **19** binds PlGF-1 with 3 log potency increase over phage-derived peptides. (a) A competitive inhibitor of the PlGF/VEGFR-1 interaction (**15**) was evolved from phage display hits. (b) PlGF-specific CovX-Bodies (**19**, **20**) interact with PlGF-1 in direct binding ELISA, while an unrelated CovX-Body (**21**) and unconjugated antibody (**1**) do not. (c) Direct binding of **19**-conjugated Fab fragment in comparison to CovX-Body **19** and **1**. (d) Competition ELISA of PlGF-specific CovX-Bodies versus **1** and soluble VEGFR-1. Triplicate samples are shown.

Table 2. Bioconjugation and Lysine Substitution[a]

compd	IC_{50} (nM)	K_D (nM)	1	2	3	4	5	6	7	8	9	10	11	12	13	14	15	16
15	1000	1000	F	D	V	C	K	W	V	T	L	P	H	C	K	V	M	
19	2	4	F	D	V	C	K	W	V	T	L	P	H	C	K	V	M	K_{AZD}
20	1000	200	$_{AZD}$F	D	V	C	K	W	V	T	L	P	H	C	K	V	M	
21		NA	$_{C}$(K_{AZD}	R	G	D	f)											
22	4	5	F	D	V	C	N	W	V	T	L	P	H	C	K_{Ac}	K_{AZD}	M	
23		8	F	D	V	C	K_{Ac}	W	V	T	L	P	H	C	K_{Ac}	V	K_{AZD}	
24		5	F	D	V	C	N	W	V	T	L	P	H	C	K_{Ac}	V	K_{AZD}	

[a] NA denotes no activity observed.

the addition of a third lysine, necessitating an orthogonal protection/deprotection strategy for incorporation of the linker during solid phase synthesis. The tethered peptide was then conjugated to the **1** antibody. In PlGF-1 direct binding ELISA (Figure 2b), the C-terminally tethered **15** variant (Table 2, **19**) demonstrated a 2 log higher binding affinity (2 nM) relative to the N-terminally tethered version (**20**, 200 nM), consistent with the orientation of peptide presentation by M13 phage.[17] These data are also consistent with previous reports of 2−3 log, avidity-driven potency increases resulting from therapeutic bivalency against a homodimer target.[18,19] Both unrelated CovX-Body **21** and the unconjugated **1** scaffold exhibited K_D values greater than 10 μM. Comparing the **19** CovX-Body with a Fab fragment conjugated with the same peptide yielded a 200 nM K_D value for the Fab (Figure 2c), suggesting potency between those of the CovX-Body and the native peptide. Relative CovX-Body potencies were reproducible in PlGF/VEGFR-1 competition ELISA (Figure 2d); **19** demonstrated an IC_{50} of 2 nM, similar to that of soluble VEGFR-1, while the IC_{50} of **20** was 1 μM, comparable with that of the native peptide. **1** is inactive as expected.

CovX-Bodies Are Specific to PlGF-1. We assessed the cross-reactivity of **19** against PlGF-2 and murine PlGF as well as VEGF and PDGF-BB, the two family members with highest homology to PlGF. In contrast to its high affinity for PlGF-1, **19** exhibited a K_D of 100 nM against PlGF-2 (Figure 3a) and of 400 nM against murine PlGF (Figure 3b). **1** was inactive against both proteins as expected. In competition ELISA, **19** inhibited the PlGF-2/VEGFR-1 interaction with an IC_{50} of approximately 150 nM, similar to its K_D (Figure 3c). While soluble murine VEGFR-1 (smVEGFR-1) could inhibit the interaction between murine PlGF and human VEGFR-1 (Figure 3d, IC_{50} = 1.4 nM), **19** was completely inactive and comparable with **1**. **19** was also unable to compete with murine PlGF binding to murine VEGFR-1, despite comparable activities and detection of all proteins tested (not shown). Binding results were comparable using SPR analyses with a closely related CovX-Body, **22** (Table 2). Moreover, SPR using **22** against PlGF-1 and PlGF-2 in comparison with VEGF and PDGF-BB demonstrated a complete lack of binding to the latter two proteins (Figure 3e).

Alteration of CovX-Body Linking Positions Confers Minimal in Vivo Stability Benefits. Using a PlGF-binding PK ELISA for assessment of **19**, we observed only 5% of functional PlGF-binding CovX-Body remaining after 6 h, with a β-phase half-life that was too short to model (Figure 4a). In contrast, IgG

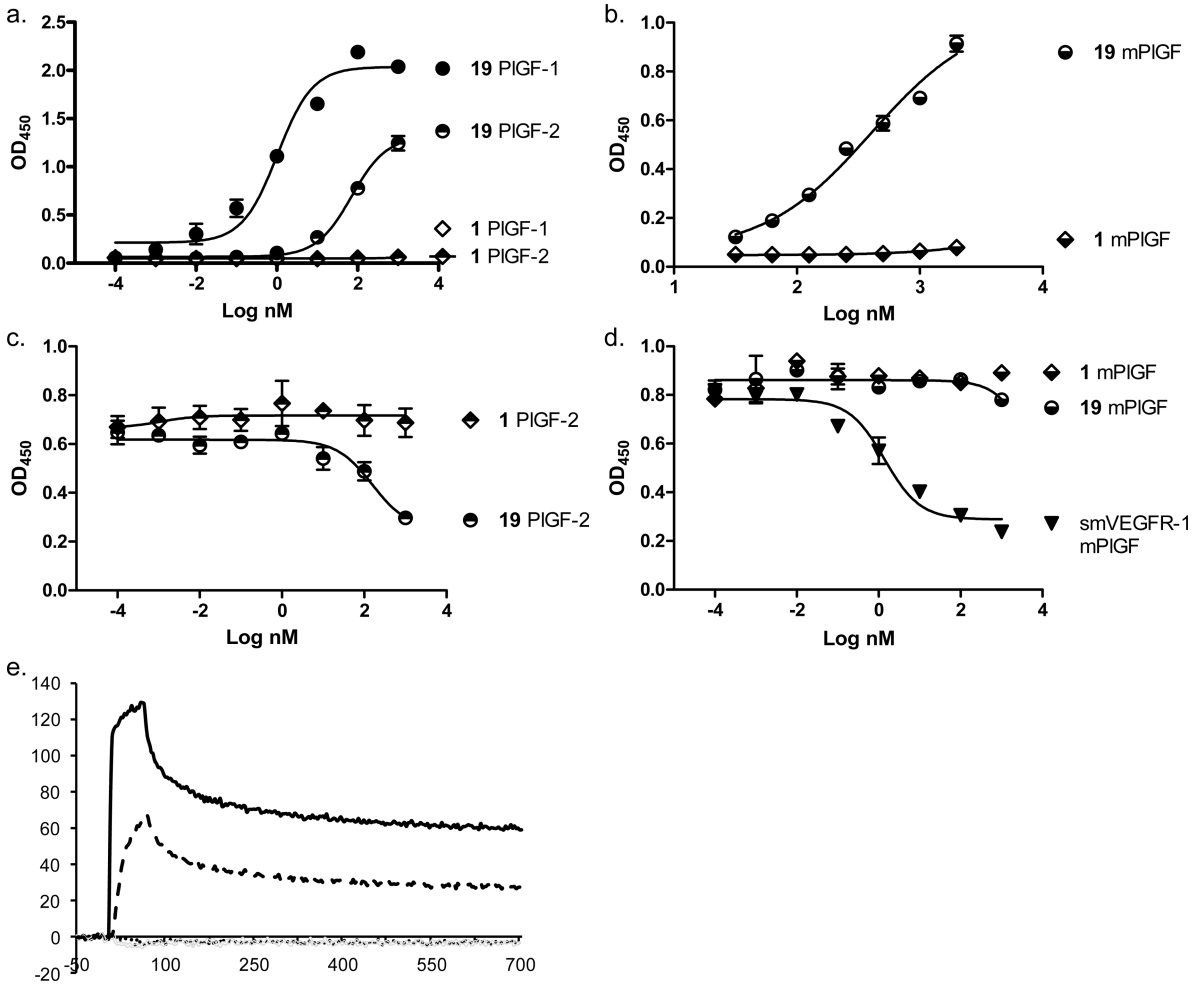

Figure 3. CovX-Bodies are specific to PlGF-1. (a) Comparison of PlGF-1 versus PlGF-2 binding by **19** and **1**. (b) Comparison of murine PlGF binding by **19** versus **1**. (c) Competition ELISA comparing inhibition of PlGF-1/hVEGFR-1 versus PlGF-2/hVEGFR-1 interactions by **19** and **1**. (d) Competition ELISA comparing inhibition of mPlGF/hVEGFR-1 interactions by **19** versus **1** and soluble murine VEGFR-1 (smVEGFR-1). Triplicate samples are shown. (e) SPR analysis comparing binding of **22** CovX-Body to PlGF-1 (solid line), PlGF-2 (dashed line), human VEGF-A (gray line), or human PDGF-BB (dotted line).

ELISA demonstrated that the antibody portion of the CovX-Body remained intact over this time period, suggesting that the loss of PlGF-binding reflected peptide instability rather than total antibody loss.

Prior to further modifications for increased stability, we first substituted Lys5 and Lys13 of **19** (Table 2). These changes, leaving only one free lysine per compound for AZD tethering, expedited peptide synthesis and greatly improved yields. The resultant compounds (**23** and **24**) retained potency relative to **19** (Table 2) but did not affect PK (not shown).

To identify the optimal pharmacophore linking position for CovX-Body stability, we generated a series of AZD tether position variants, a "tether walk" (Table 3). In agreement with phage conservation of the Leu-Pro-His motif at positions 9−11, a tether walk of **24** (**22**, **25**−**31**) revealed that these residues were not permissive linker attachment sites despite tolerance of Ala10 in lieu of Pro10 (**11**). Indeed, only tethering at the C-terminal residues 13−15 or at a single residue within the disulfide ring (position 8) retained potency (Figure 4b, underlined). A CovX-Body tethered at position 8 ("mid-linked", **29**) yielded 20% of functional molecule remaining at 6 h versus less than 5% of **22** ("C-terminally tethered").

Concurrently, screening of focused phage libraries based on initial hit **3** yielded peptide **37** (Table 3) as a PlGF/VEGFR-1 antagonist (IC_{50} = 400 nM). A tether walk of **37** (not shown) reiterated that of **24**, and its mid-linked variant (**38**) exhibited subnanomolar potency (Table 3). **38** was also specific to human PlGF-1 over PlGF-2 and mouse PlGF (not shown) but exhibited PK comparable with that of **24** (<5% remaining at 6 h).

In Vivo Cleavage of Biotinylated Peptides Suggests Peptide Instability at the C Terminus. To identify the primary peptide cleavage sites, an in vivo PK assessment was executed using nine biotinylated variants of the same CovX-Body. The biotin moiety was selected because it is readily bioconjugated and offers a highly sensitive method of detection irrespective of peptide activity. N-Terminally, mid-linked, or C-terminally tethered variants of **23** (Table 1S in Supporting Information) were biotinylated once per compound at the N-, mid-, or C-terminus (Figure 4d, Figure 4f, Figure 4h), and mice were dosed to permit in vivo cleavage at labile sites.

Modified ELISAs measured the presence of biotin rather than binding to PlGF; consequently, the assay was an unbiased measurement of site-specific peptide cleavage independent of biological activity. Data were normalized for the IgG levels in each

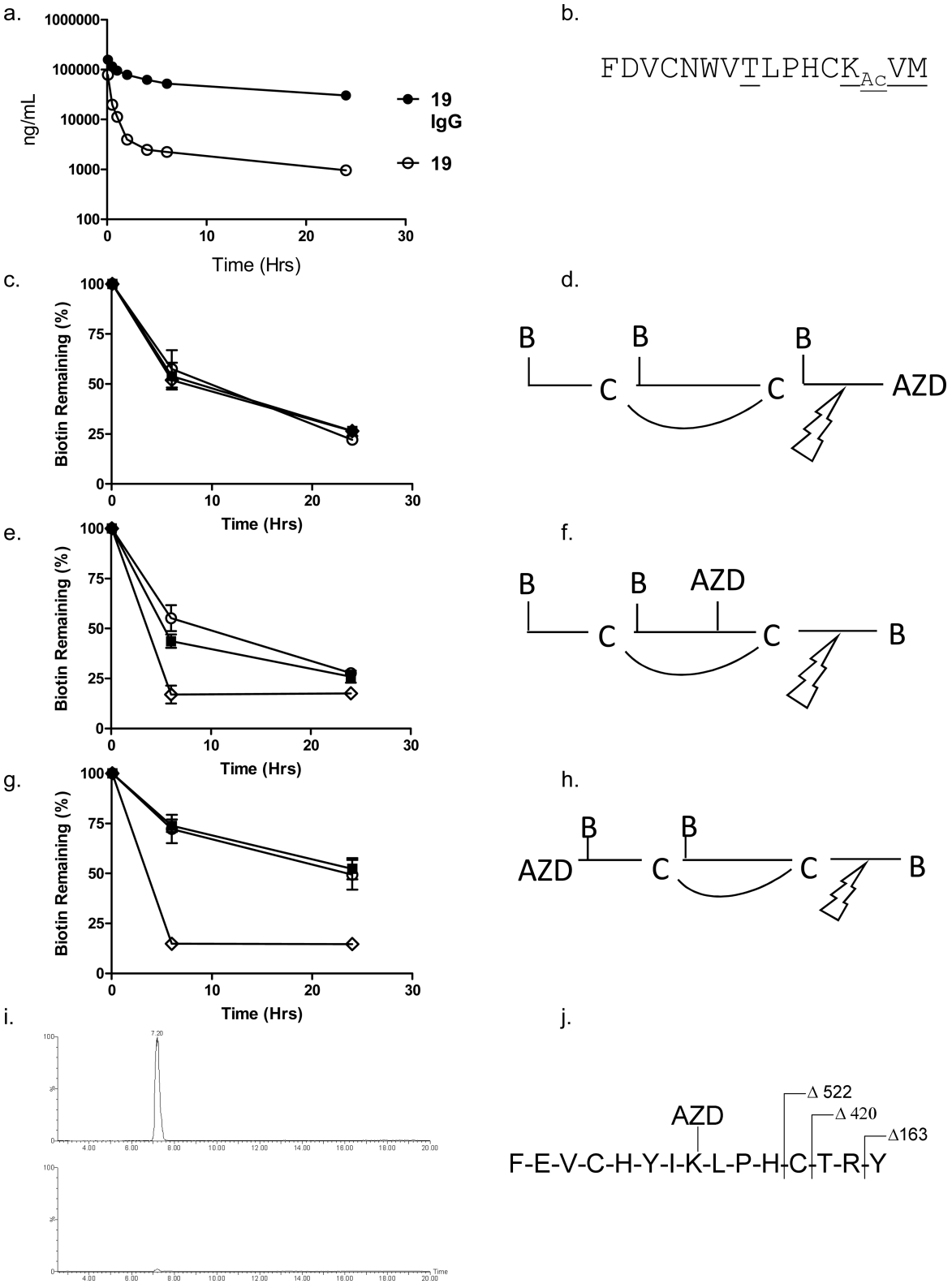

Figure 4. Identification of CovX-Body proteolytic hotspots. (a) PK of PlGF-binding **19** (open circles) versus antibody IgG levels (filled circles) in male CFW mice over 24 h. Triplicate samples are shown. (b) Restricted and permitted (underlined) residues for antibody conjugation, as determined by retention or loss of PlGF binding. Results are shown for **24**. (c−h) Biotinylated compound determination of C-terminal cleavage of lead peptides. Compounds were biotinylated at the C terminus (open diamonds), within the disulfide ring (filled squares) or at the N terminus (open circles). Data shown for C-terminally tethered (c), mid-linked (e), or N-terminally tethered (g) compounds are the percent of original biotin remaining at indicated time points following normalization for IgG levels. Suggested peptide cleavage site as indicated by kinetics of biotin (B) loss for C-terminally tethered (d), mid-linked (f), or N-terminally tethered (h) compounds. (i) Loss of predominant peptide species of **38** in cathepsin B incubated (bottom) versus control (top) samples. (j) Cathepsin B cleavage sites as indicated by LCMS analysis of **38** kinetics study.

dx.doi.org/10.1021/jm101226k |*J. Med. Chem.* 2011, 54, 1256–1265

Table 3. Tether Walk and D-Amino Acid Incorporation

compd	IC_{50} (nM)	K_D (nM)	1	2	3	4	5	6	7	8	9	10	11	12	13	14	15	functional at 6 h (%)
24		5	F	D	V	C	N	W	V	T	L	P	H	C	K_{Ac}	V	K_{AZD}	
22	4	5	F	D	V	C	N	W	V	T	L	P	H	C	K_{Ac}	K_{AZD}	M	<5
25	54	4	F	D	V	C	N	W	V	T	L	P	H	C	K_{AZD}	V	M	11
26	>1000	>1000	F	D	V	C	N	W	V	T	L	P	K_{AZD}	C	K_{Ac}	V	M	
27	>1000	>1000	F	D	V	C	N	W	V	T	L	K_{AZD}	H	C	K_{Ac}	V	M	
28	>1000	>1000	F	D	V	C	N	W	V	T	K_{AZD}	P	H	C	K_{Ac}	V	M	
29	4	9	F	D	V	C	N	W	V	K_{AZD}	L	P	H	C	K_{Ac}	V	M	20
30	>1000	>1000	F	D	V	C	N	W	K_{AZD}	T	L	P	H	C	K_{Ac}	V	M	
31	>1000	>1000	F	D	V	C	N	K_{AZD}	V	T	L	P	H	C	K_{Ac}	V	M	
32	624	6	F	D	V	C	K_{AZD}	W	V	T	L	P	H	C	K_{Ac}	V	M	
33	>1000	>1000	F	D	K_{AZD}	C	N	W	V	T	L	P	H	C	K_{Ac}	V	M	
34		>1000	F	K_{AZD}	V	C	N	W	V	T	L	P	H	C	K_{Ac}	V	M	
35		>1000	K_{AZD}	D	V	C	N	W	V	T	L	P	H	C	K_{Ac}	V	M	
36		>1000	F_{AZD}	D	V	C	N	W	V	T	L	P	H	C	K_{Ac}	V	M	
37	400		F	E	V	C	H	Y	I	R	L	P	H	C	T	R	Y	
38	0.7	0.3	F	E	V	C	H	Y	I	K_{AZD}	L	P	H	C	T	R	Y	4
39	0.2		F	E	V	C	H	Y	I	K_{AZD}	L	P	H	C	t	R	Y	23

Table 4. Potency and PK of Lead PlGF-Targeting CovX-Bodies

compd	IC_{50} (nM)	K_D (nM)	leader	1	2	3	4	5	6	7	8	9	10	11	12	13	14	15	murine β $t_{1/2}$ (h)
40	1	0.3	DAA	F	E	V	C	H	Y	I	K_{AZD}	L	P	H	C	t	r	y	14
41	3	8	ADAA	F	E_{Me}	V	C	H	Y	I	K_{AZD}	L	Aib	H	C	t	r	y	24
2	0.4	0.1	ADAA	F	E_{Me}	V	C	H	Y	I	K_{AZD}	L	Aib	H	C	t	K_{Ac}	Aib	75

case. These levels were consistent with those observed for nonbiotinylated molecules in PK experiments (Figure 1S), suggesting that the presence of biotin did not lead to different total antibody processing in vivo.

As evident in Figure 4c, all C-terminally tethered compounds demonstrated identical cleavage kinetics relative to each other with approximately 50% biotin loss at 6 h and 80% loss at 24 h. These compounds also exhibited the slowest loss of the C-terminal biotin relative to other tether sites (compare **4c** with **4e** and **4g**), suggesting partial protection by C-terminal conjugation. While in vivo masking of the biotin moieties cannot be strictly ruled out, the data indicate a predominant cleavage site near the peptide's C terminus, between the tether site and its closest biotin (Figure 4d). Mid-linked compounds (Figure 4e) demonstrated a more rapid loss of the C-terminal site, with 80% loss at 6 h. This result was consistent with PK data for mid-linked CovX-Body **29** and also suggested cleavage C-terminal to the tether (Figure 4f). N-Terminally tethered compounds (Figure 4g) exhibited a very rapid C-terminal loss, with an 80% loss at 6 h, and the slowest loss of N-terminal biotins relative to other tether spots (compare **4g** with **4c** and **4e**). This result was consistent with relative protection of the N terminus by the attached antibody and lack of protection at the C terminus, again suggesting the same C-terminal cleavage area (Figure 4h). Together, the data strongly indicated that the section of the peptide between the second cysteine and the C terminus was the most labile region, with tethering in that region affording minimal protease protection.

In Vitro Cathepsin B Cleavage Correlates with in Vivo PK and Identifies Proteolytic Hotspots at the C Terminus. In parallel, in vitro cleavage with the lysosomal protease cathepsin B was assessed. Consistent with the in vivo instability of CovX-Body **38**, the tethered **38** peptide was susceptible to cleavage by cathepsin B (Figure 4i), as indicated by the loss of the major species eluting at 7.80 min in cathepsin B cleaved (bottom) versus control (top) samples. Kinetic analyses (not shown) revealed that **38** is a competitive inhibitor of known cathepsin B substrates. Moreover, the sequential loss of 163, 420, and 522 Da fragments, corresponding to the C-terminal residues, indicates that **38** is progressively degraded from the C terminus (Figure 4j). Together, the biotin walk and cathepsin B studies indicated primary peptide cleavage at the C terminus. In support of this hypothesis, incorporation of a single D-amino acid at position 13 of **38** (**39**) increased percent remaining at 6 h from 4% to 23% (Table 3).

Optimized CovX-Body 2 Exhibits Enhanced Potency and Stability Conferred via Directed Modifications. D-Amino acid substitution at any single residue along the **38** peptide was not tolerated for retention of binding with the exception of the three C-terminal residues (Thr13, Arg14, and Tyr15). To further stabilize this labile region, D-amino acids were incorporated at all three of these residues. Concurrently, to eliminate any additional exopeptidase activity, we incorporated extensions to the N terminus based upon the leader sequence incorporated by M13 phage. Together, these changes improved the percent remaining at 24 h to 15% and enabled a β half-life determination of approximately 14 h (**40**, Table 4). Substituting Glu with *N*-methyl Glu (E_{Me}) and substituting Aib at the LPH-motif proline residue yielded **41**, which demonstrated a β phase half-life of 24 h. Finally, substituting the penultimate D-Arg with Lys(Ac) and the C-terminal D-Tyr with Aib yielded optimized CovX-Body **2**.

2 exhibited more potent binding to PlGF-1 (Figure 5a) and competition with VEGFR-1 (Figure 5b) than **19** (K_D = 0.1 nM

dx.doi.org/10.1021/jm101226k | J. Med. Chem. 2011, 54, 1256–1265

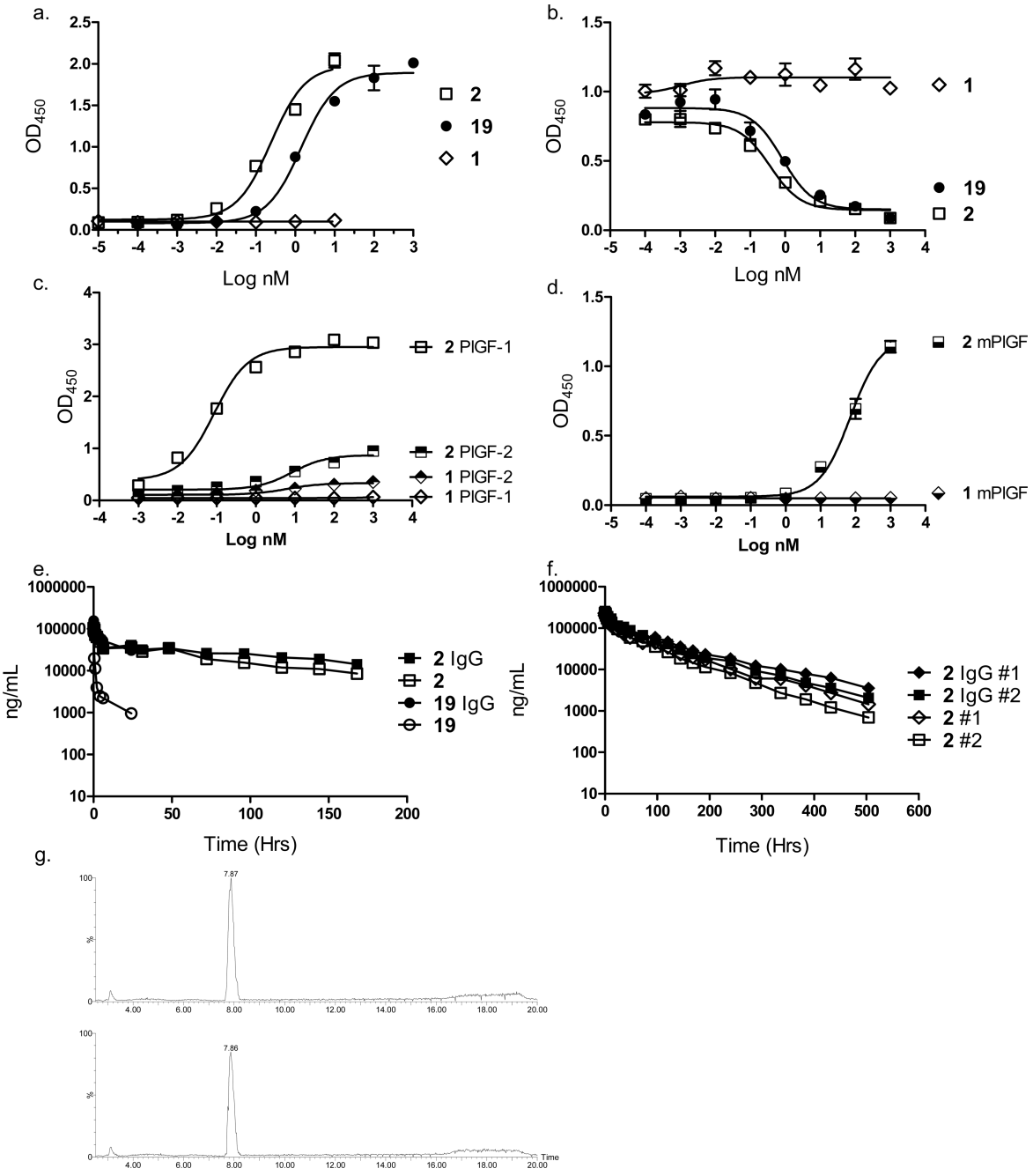

Figure 5. Lead CovX-Body **2** retains potency of **19** and exhibits scalable, stable pharmacokinetics in mouse and non-human primate. (a) Direct PlGF-1 binding ELISA comparing **2** to **19**. (b) PlGF-1/VEGFR1 competition ELISA comparing **2** to **19**. (c) Direct binding of **2** to PlGF-1 versus PlGF-2. (d) Direct binding of **2** to murine PlGF. (e) PK of **2** versus **19** and accompanying IgG levels in male CFW mice. (f) PK of **2** and accompanying IgG levels in two male cynomolgus monkeys. Data from each monkey are shown independently in duplicate. (g) LCMS analysis of control (top) versus cathepsin B incubated (bottom) **2**.

versus 3.5 nM and IC_{50} = 0.4 nM versus 2 nM, Tables 2 and 4). Similar to **19**, binding of **2** to PlGF-2 and to mouse PlGF was much weaker than that to PlGF-1; a K_D of 9 nM for PlGF-2 binding (Figure 5c) and a K_D of 70 nM for mPlGF binding (Figure 5d) were observed. **2** demonstrated dramatically increased stability relative to **19**, with a β half-life of approximately 75 h in mouse and very little loss of peptide versus antibody over a 7 day study (Figure 5e, Table 2). These data were comparable with those observed in cynomolgus monkey, which in two animals yielded an average β half-life of 78 h (Figure 5f). As observed in mice, functional CovX-Body levels (filled diamonds, squares) tracked closely with the total antibody levels (open diamonds, squares).

Correlating with its PK in vivo, the **2** peptide was resistant to in vitro cleavage by cathepsin B, as indicated by retention of the major peptide species eluting at 8.56 min following cathepsin B incubation (Figure 5g). CovX-Body **40**, known to have in vivo PK between those of **38** and **2** (Tables 3 and 4), also demonstrated intermediate kinetics of in vitro cathepsin B cleavage (not shown).

dx.doi.org/10.1021/jm101226k |*J. Med. Chem.* 2011, 54, 1256–1265

DISCUSSION

Conjugation of peptides to the **1** scaffold yields bivalent therapeutics structurally resembling antibodies;[3] thus, a 2-fold potency difference between native peptide and CovX-Body is expected upon peptide-to-CovX-Body conjugation. The 1000-fold difference in PlGF-1 binding affinity observed here reflects additional potency possibly offered by avidity. One can hypothesize that the multivalency of M13 phage may have supported selection for this. The avidity lent by the bivalent CovX-Body is also interesting given that PlGF is a homodimer.

The discovery of therapeutic peptides using phage display faces the challenge that screening for target affinity does not necessarily select for molecules that are biologically stable. Conjugation to macromolecular carriers and the incorporation of D-amino acids have been successfully applied to extend half-lives of peptides in vivo.[13,20] While stability benefits were observed here from these approaches, additional benefits were conferred by substituting D-amino acids with other unnatural moieties. Lead CovX-Body **2** is identical to precursor **41** except for the presence of Lys(Ac) and Aib in lieu of two D-amino acids at a region of the peptide critical to stability; yet its β half-life in vivo is 50 h longer. Thus, the data presented here suggest that D-amino acids, generally considered resistant to proteolysis, can indeed be labile.

2 exhibits PK and potency that should support once-weekly dosing in efficacy models. A mean serum concentration of approximately 15 000 ng/mL was observed 168 h after 10 mg/kg dosing in the non-human primate. Given PlGF plasma levels of 100 pg/mL, conservatively, the expected molar excess of CovX-Body to target is approximately 6×10^4 after 7 days. This vast molar excess of CovX-Body to target in circulation is accompanied by a 0.1 nM affinity for PlGF, comparable with that of its receptor, VEGFR-1.[16] Thus, **2** is likely to function as a competitive inhibitor in vivo.

The specific binding of **2** to PlGF-1 over the longer splice variant PlGF-2[21] may suggest binding to an epitope masked by the heparin binding domain of PlGF-2. Crystal structures of PlGF in complex with VEGFR-1 lack this domain;[16,22] thus, information regarding its influence on other surfaces of the molecule is lacking. However, because the heparin binding region permits the interaction of VEGFR-1 with VEGFR-2 and with the neuropilins,[8,10] the specific biological roles of PlGF-1 versus PlGF-2 may be markedly different; information to this end is also incomplete. Furthermore, because only one PlGF is expressed in mouse and because that protein is more homologous to PlGF-2, the failure to recognize PlGF-1 as a potentially key component may lead to misinterpretations between mouse and human PlGF biology. The biology of this axis is complicated even further given that VEGFR-1 interacts with VEGF proteins and that mouse and human PlGF and VEGFR-1 can efficiently cross-interact in xenograft models.[5]

Recent, highly conflicting data using two panels of PlGF-targeting antibodies have underscored current questions around PlGF biology.[11−13] Moreover, they may call into question the suitability of PlGF as a human cancer target. In combination with the mPlGF, PlGF-1/2, and mPlGF/hPlGF-2 targeting molecules previously reported, the PlGF-1-specific CovX-Body described here permits a more thorough delineation of PlGF biology than previously feasible. Moreover, these studies should elucidate the relative contribution of murine versus human PlGF to xenograft growth, thus also providing insight into the clinical relevance of these models with respect to anti-PlGF therapies.

EXPERIMENTAL SECTION

Peptide Synthesis. Rink amide resin (Polymers Labs) was swelled in DMF. Fmoc-protected amino acids (EMD Biosciences), solvents (EMD Biosciences), and reagents (Sigma-Aldrich) were used in conventional Fmoc chemistries on a PTI Symphony parallel synthesizer. Peptides were released from polymer support using a universal cleavage cocktail (85:5:5:2.5:2.5, TFA/PhOH/DTT/TIPS/H_2O). Crude peptides were precipitated with cold diethyl ether, dissolved in methanol, and oxidized with iodine. Lysine residues of oxidized peptides were coupled to NHS-activated tethers in the presence of NMM. Peptides were purified by reverse phase HPLC on Phenomenex preparative Luna C18 columns using 0.1% TFA in H_2O and 0.1% TFA in ACN gradients and lyophilized. All peptides were validated for 95% purity and mass by analytical LCMS. Accurate masses were analyzed using a Waters Synapt G2 Q-Tof mass spectrometer.

CovX-Body Conjugation. Tethered compounds were conjugated with **1** (3:1 ratio, peptide/**1**), purified by size exclusion gel chromatography on an AKTA FLPC system, buffer exchanged, and concentrated in PBS. Concentrations were measured by UV absorbance at OD_{280}. Conjugation was characterized by LCMS analysis; all CovX- Bodies used were 70−86% bivalent.

ELISA Reagents. rhPlGF-1 (no. 264-PG), rmPlGF (no. 465-PL), anti-human-PlGF biotinylated antibody (no. BAF264), anti-mouse PlGF biotinylated antibody (no. BAF465), rhVEGFR-1-Fc (no. 321-FL), and rmVEGFR-1-Fc (471-F1) were from R&D Systems. rhPlGF-2 (no. 4741-50) was from Biovision. ELISA wash buffer (50-63-01) and TMB SureBlue Microwell Peroxidase substrate (no. 50-63-01 or no. 52-00-00) were from KPL. Half-well high-binding ELISA plates (no. 3690) and full-well plates (no. 9018) were from Costar. Superblock (no. 2011 or AAA500) was from ScyTek. Poly-streptavidin-HRP (no. RDI-PHRP20-SA2) was from Fitzgerald Laboratories. Streptavidin-HRP (no. 554066) was from BD Pharmingen. HRP-conjugated goat anti-human IgG-F(ab)2 (no. W9-035-097) was from Jackson Immunoresearch. Anti-human IgG coating antibody (no. E80-104) and HRP-conjugated goat anti-human IgG H+L (no. A80-319P) were from Bethyl Laboratories.

ELISA. ELISAs were as follows in triplicate unless otherwise specified. Plates were coated at 1 μg/mL in PBS overnight at 4 °C and blocked using Superblock for 1 h at room temperature. Subsequent incubations were for 1 h at room temperature with dilutions in Superblock. Plates were washed 3× between steps using a Biotek ELx405 plate washer and developed using TMB substrate. Reactions were stopped in 2 M H_2SO_4 and OD_{450} values were read on a Molecular Devices SpectraMax Plus plate reader.

VEGFR-1 Competition. Half-well plates were coated with 0.5 μg/mL VEGFR1-Fc and blocked. Compounds were titrated in 50% FBS/50% Superblock containing 1 ng/mL PlGF-1. PlGF was detected using 1:1000 biotinylated anti-PlGF antibody followed by 1:1000 poly-streptavidin-HRP.

PlGF Direct Binding ELISA. For PlGF direct binding, half-well plates were coated with biotinylated anti-PlGF antibody and blocked prior to addition of 25 nM PlGF. Compounds were titrated in 50%FBS/50% Superblock and detected using 1:1000 anti-human-Fab-HRP.

PlGF-Binding PK. Full-well plates were coated with monoclonal anti-**1** idiotype and blocked prior to addition of standards/QCs (prepared using CovX-Body dosing solution) or prediluted serum samples from PK animals. All samples were in duplicate and contained 5% final mouse or monkey serum in Superblock. PlGF was used at 25 ng/mL and detected with 0.05 μg/mL biotinylated anti-PlGF antibody, followed by 1:6000 streptavidin/HRP. IgG ELISAs were identical except for detection with 1:50000 goat anti-human IgG/HRP.

Biotin Detection. Half-well plates were coated with 1:100 anti-IgG antibody in 0.05 M carbonate bicarbonate and blocked prior to titration of PK samples. Biotin was detected using 1:1000 poly-streptavidin-HRP. IgG ELISAs were identical except that **1** was detected with 1:10000 goat anti-human IgG/HRP.

SPR Analyses. SPR was performed on a ProteOn XPR36 system (BioRad) at 25 °C. Biotinylated goat anti-human IgG (Invitrogen, H10015) was captured on an NLC chip (BioRad) to 2300 RU. Analytes were diluted in PBS containing 0.005% Tween 20. 50 nM CovX-Bodies were injected at 30 μL/min for 5 min. 200 nM recombinant proteins were injected at 100 μL/min for 1 min followed by 10 min of dissociation. Surface was regenerated with two injections of 10 mM glycine, pH 2.0 (BioRad), at 100 μL/min for 18 s. Data were double-referenced to **1** surface and buffer injection using Scrubber 2 (BioLogic Software).

Cathepsin B Cleavage. An amount of 1 μg/mL cathepsin B (Biovision no. 1021-5) was incubated with DMSO or CovX-Bodies (1−50 μM) +/− cathepsin B substrates (R&D Systems no. ES008) at 0−100 μM. Then 100 μL mixtures incubated in opaque black ELISA plates were read at indicated excitation/emission wavelengths every 30 s for 30 min.

Animal Studies. All animal experiments were conducted after protocol approval by the CovX/Pfizer Institutional Animal Care and Use Committee. For mouse PK, male Swiss Webster mice (CFW, Charles Rivers, Hollister, CA) weighing 21−23 g on study start were used. Mice were acclimated to laboratory conditions for ≥48 h prior to dosing. For monkey PK, two male cynomolgus monkeys (*Macaca fascicularis*, Institute Pertanian Bogor, Indonesia) 2−4 years old and weighing 2−3 kg on study start were used. Animals were acclimated to the primate unit at the study facility (Maccine Pte Ltd., Singapore) for ≥10 days prior to dosing. All animals were dosed iv at 10 mg/kg. Blood samples were taken at the indicated time points, clotted for 30−60 min, and centrifuged at 3000 rpm (monkey) or 12 000 rpm (mouse) for 10 min at 4 °C. Serum was collected and stored at −80 °C. Data were analyzed using WinNonLin software fit to a two-compartment model.

■ ASSOCIATED CONTENT

Ⓢ Supporting Information. C18 RP-HP-LCMS conditions, RP-HPLC−MS retention times and accurate masses found, representative IgG levels for biotinylated versus nonbiotinylated molecules, characterization data for compound **2**. This material is available free of charge via the Internet at http://pubs.acs.org.

■ AUTHOR INFORMATION

Corresponding Author

*For K.E.B.: phone, (858)964-2030; fax, (858)964-2090; e-mail, kristen.e.bower@pfizer.com. For S.N.L.: phone, (858)964-2074; fax, (858) 964-2090; e-mail, son.lam@pfizer.com.

Present Addresses

‡Sanford-Burnham Medical Research Institute, 10901 North Torrey Pines Road, San Diego, CA 92037.

§Traversa Therapeutics, Inc. 10480 Wateridge Circle, San Diego, CA. 92121.

Author Contributions

†These authors contributed equally to this work.

■ ABBREVIATIONS USED

PlGF, placenta/placental growth factor; VEGFR-1, VEGF receptor 1; ELISA, enzyme-linked immunosorbant assay; SAR, structure−activity relationship; FcRn, neonatal Fc receptor; Flk-1, fetal liver kinase 1; Flt-1, fms-related tyrosine kinase 1; α-PlGF, anti-PlGF/α-PlGF; mAb, monoclonal antibody; hPlGF, human PlGF; mPlGF, murine PlGF; sVEGFR-1, soluble VEGFR-1; AZD, azetidin-2-one; PDGF-BB, platelet-derived growth factor BB; rhPlGF, recombinant human PlGF; rmPlGF, recombinant murine PlGF; TMB, tetramethylbenzidine; HRP, horseradish peroxidase; SPR, surface plasma resonance; iv, intraveneous; PK, pharmacokinetics

■ REFERENCES

(1) McGregor, D. P. Discovering and improving novel peptide therapeutics. *Curr. Opin. Pharmacol.* **2008**, *8*, 616–619.

(2) Schroeder, H. W., Jr.; Cavacini, L. Structure and function of immunoglobulins. *J. Allergy Clin. Immunol.* **2010**, *125*, S41–S52.

(3) Woodnutt, G.; Violand, B.; North, M. Advances in protein therapeutics. *Curr. Opin. Drug Discovery Dev.* **2008**, *11*, 754–761.

(4) Mendelson, D. S.; Dinolfo, M.; Cohen, R. B.; Rosen, L. S.; Gordon, M. S.; Byrnes, B.; Bear, I.; Schoenfeld, S. L. First-in-human dose escalation safety and pharmacokinetic (PK) trial of a novel intravenous (IV) thrombospondin-1 (TSP-1) mimetic humanized monoclonal CovX-Body (CVX-045) in patients (pts) with advanced solid tumors. *J. Clin. Oncol.* **2008**, *26* (15S), 3524.

(5) Fischer, C.; Mazzone, M.; Jonckx, B.; Carmeliet, P. FLT1 and its ligands VEGFB and PlGF: drug targets for anti-angiogenic therapy? *Nat. Rev. Cancer* **2008**, *8*, 942–956.

(6) Sawano, A.; Takahashi, T.; Yamaguchi, S.; Aonuma, M.; Shibuya, M. Flt-1, but not KDR/Flk-1 tyrosine kinase is a receptor for placenta growth factor, which is related to vascular endothelial growth factor. *Cell Growth Differ.* **1996**, *7*, 213–221.

(7) Persico, M. G.; Vincenti, V.; DiPalma, T. Structure, expression and receptor-binding properties of placenta growth factor (PlGF). *Curr. Top. Microbiol. Immunol.* **1999**, *237*, 31–40.

(8) Park, J. E.; Chen, H. H.; Winer, J.; Houck, K. A.; Ferrara, N. Placenta growth factor: potentiation of vascular endothelial growth factor bioactivity in vitro and in vivo and high affinity binding to Flt-1 but not Flk-1/KDR. *J. Biol. Chem.* **1994**, *269*, 25646–25654.

(9) Autiero, M.; Waltenberger, J.; Communi, D.; Kranz, A.; Moons, L.; Lambrechts, D.; Kroll, J.; Plaisance, S.; De Mol, M.; Bono, F.; Kliche, S.; Fellbrich, G.; Ballmer-Hofer, K.; Maglione, D.; Mayr-Beyrle, U.; Dewerchin, M.; Dombrowski, S.; Stanimirovic, D.; Van Hummelen, P.; Dehio, C.; Hicklin, D. J.; Persico, G.; Herbert, J. M.; Communi, D.; Shibuya, M.; Collen, D.; Conway, E. M.; Carmeliet, P. Role of PlGF in the intra- and intermolecular cross talk between the VEGF receptors Flt1 and Flk1. *Nat. Med.* **2003**, *9*, 936–943.

(10) Migdal, M.; Huppertz, B.; Tessler, S.; Comforti, A.; Shibuya, M.; Reich, R.; Baumann, H.; Neufeld, G. Neuropilin-1 is a placenta growth factor-2 receptor. *J. Biol. Chem.* **1998**, *273*, 22272–22278.

(11) Fischer, C.; Jonckx, B.; Mazzone, M.; Zacchigna, S.; Loges, S.; Pattarini, L.; Chorianopoulos, E.; Liesenborghs, L.; Koch, M.; De Mol, M.; Autiero, M.; Wyns, S.; Plaisance, S.; Moons, L.; van Rooijen, N.; Giacca, M.; Stassen, J. M.; Dewerchin, M.; Collen, D.; Carmeliet, P. Anti-PlGF inhibits growth of VEGF(R)-inhibitor-resistant tumors without affecting healthy vessels. *Cell* **2007**, *131*, 463–475.

(12) Van de Veire, S.; Stalmans, I.; Heindryckx, F.; Oura, H.; Tijeras-Raballand, A.; Schmidt, T.; Loges, S.; Albrecht, I.; Jonckx, B.; Vinckier., S.; Van Steenkiste, C.; Tugues, S.; Rolny, C.; De Mol, M.; Dettori, D.; Hainaud, P.; Coenegrachts, L.; Contreres, J. O.; Van Bergen, T.; Cuervo, H.; Xiao, W. H.; Le Henaff, C.; Buysschaert, I.; Kharabi Masouleh, B.; Geerts, A.; Schomber, T.; Bonnin, P.; Lambert, V.; Haustraete, J.; Zacchigna, S.; Rakic, J. M.; Jiménez, W.; Noël, A.; Giacca, M.; Colle, I.; Foidart, J. M.; Tobelem, G.; Morales-Ruiz, M.; Vilar, J.; Maxwell, P.; Vinores, S. A.; Carmeliet, G.; Dewerchin, M.; Claesson-Welsh, L.; Dupuy, E.; Van Vlierberghe, H.; Christofori, G.; Mazzone, M.; Detmar, M.; Collen, D.; Carmeliet, P. Further pharmacological and genetic evidence for the efficacy of PlGF inhibition in cancer and eye disease. *Cell* **2010**, *141*, 178–190.

(13) Bais, C.; Wu, X.; Yao, J.; Yang, S.; Crawford, Y.; McCutcheon, K.; Tan, C.; Kolumam, G.; Vernes, J. M.; Eastham-Anderson, J.; Haughney, P.; Kowanetz, M.; Hagenbeek, T.; Kasman, I.; Reslan, H. B.; Ross, J.; Van Bruggen, N.; Carano, R. A.; Meng, Y. J.; Hongo, J. A.; Stephan, J. P.; Shibuya, M.; Ferrara, N. PlGF blockade does not inhibit angiogenesis during primary tumor growth. *Cell* **2010**, *141*, 166–177.

(14) Bae, D. G.; Kim, T. D.; Li, G.; Yoon, W. H.; Chae, C. B. Anti-flt-1 peptide, a vascular endothelial growth factor receptor-1-specific hexapeptide, inhibits tumor growth and metastasis. *Clin. Cancer Res.* **2005**, *11*, 2651–2661.

(15) Wu, Y.; Zhong, Z.; Huber, J.; Bassi, R.; Finnerty, B.; Corcoran, E.; Li, H.; Navarro, E.; Balderes, P.; Jimenez, X.; Koo, H.; Mangalampalli, V. R.; Ludwig, D. L.; Tonra, J. R.; Hicklin, D. J. Anti-vascular endothelial growth factor receptor-1 antagonist antibody as a therapeutic agent for cancer. *Clin. Cancer Res.* **2006**, *12*, 6573–6584.

(16) Christinger, H. W.; Fuh, G.; de Vos, A. M.; Wiesmann, C. The crystal structure of placental growth factor in complex with domain 2 of vascular endothelial growth factor receptor-1. *J. Biol. Chem.* **2004**, *279*, 10382–10388.

(17) Barbas, C. F. III.; Burton, D. R.; Scott, J. K.; Silverman, G. J. *Phage Display: A Laboratory Manual*; Cold Spring Harbor Laboratory Press: Cold Spring Harbor, NY, 2001.

(18) Radnai, L.; Rapali, P.; Hodi, Z.; Suveges, D.; Molnar, T.; Kiss, B.; Becsi, B.; Erdodi, F.; Buday, L.; Kardos, J.; Kovacs, M.; Nyitra, L. Affinity, avidity and kinetics of target sequence binding to LC8 dynein light chain isoforms. *J. Biol. Chem.* **2010**, *285*, 38649−38657.

(19) Chen, W.; Xiao, X.; Wang, Y.; Zhu, Z.; Dimitrov, D. S. Bifunctional fusion proteins of the human engineered antibody domain m36 with human soluble CD4 are potent inhibitors of diverse HIV-1 isolates. *Antiviral Res.* **2010**, *88*, 107–115.

(20) Tugyi, R.; Uray, K.; Iván, D.; Fellinger, E.; Perkins, A.; Hudecz, F. Partial D-amino acid substitution: improved enzymatic stability and preserved Ab recognition of a MUC2 epitope peptide. *Proc. Natl. Acad. Sci. U.S.A.* **2005**, *102*, 413–418.

(21) Maglione, D.; Guerriero, V.; Viglietto, G.; Ferraro, M. G.; Aprelikova, O.; Alitalo, K.; Del Vecchio, S.; Lei, K. J.; Chou, J. Y.; Persico, M. G. Two alternative mRNAs coding for the angiogenic factor, placenta growth factor (PlGF), are transcribed from a single gene of chromosome 14. *Oncogene* **1993**, *8*, 925–931.

(22) Iyer, S.; Leonidas, D. D.; Swaminathan, G. J.; Maglione, D.; Battisti, M.; Tucci, M.; Persico, M. G.; Acharya, K. R. The crystal structure of human placenta growth factor 1 (PlGF-1), an angiogenic protein, at 2.0 Å resolution. *J. Biol. Chem.* **2001**, *276*, 12153–12161.